Ma, Yuchen; Lehtinen, P.O.; Foster, A. S.; Nieminen, R. M.

Hydrogen-induced magnetism in carbon nanotubes

Published in:
Physical Review B

DOI:
10.1103/PhysRevB.72.085451

Published: 01/01/2005

Document Version
Publisher's PDF, also known as Version of record

Please cite the original version:
Ma, Y., Lehtinen, P. O., Foster, A. S., & Nieminen, R. M. (2005). Hydrogen-induced magnetism in carbon nanotubes. Physical Review B, 72(8), 1-6. [085451]. https://doi.org/10.1103/PhysRevB.72.085451

Hydrogen-induced magnetism in carbon nanotubes

Yuchen Ma,* P. O. Lehtinen, A. S. Foster, and R. M. Nieminen
Laboratory of Physics, Helsinki University of Technology, P.O. Box 1100, Helsinki 02015, Finland
(Received 18 March 2005; revised manuscript received 17 June 2005; published 24 August 2005)

Spin-polarized density functional theory is used to investigate hydrogen-induced magnetism in single-walled carbon nanotubes (SWNTs). Hydrogen trapped at a carbon vacancy can trigger delocalized π electron spin polarization on semiconducting zigzag SWNTs. Hydrogen pinned by a carbon adatom on the surface of the SWNT can induce spin polarization localized at the carbon adatom, independent of the diameter and chirality of the tube.

DOI: 10.1103/PhysRevB.72.085451 PACS number(s): 61.46.+w, 61.72.Ji, 75.50.Dd

I. INTRODUCTION

There has been rapid progress in the study of the magnetism of carbon-based materials due to their potential applications. Ferro- and ferrimagnetism have been experimentally observed in rhombohedral C_{60} (Rh-C_{60}),[1] activated carbon fibers,[2] and proton-irradiated graphite.[3] The origin of magnetism in these materials is still an open question. Theoretically, dangling bonds associated with the defects,[4–6] states localized on edge-carbon atoms,[7,8] and negative Gaussian curvature[9] have been considered as the possible origins of magnetism.

Suggestions to induce magnetism in carbon nanotubes include introducing defects,[10,11] cutting nanotubes into finite lengths,[5,12] and contacting nanotubes to a magnetic substrate.[13] During growth and under ion irradiation, defects will inevitably appear in carbon nanotubes,[14,15] with vacancies and carbon adatoms as two of the dominant defect species. In our previous work,[6,10,11] we have found that vacancies and adatoms can induce magnetism in carbon nanotubes. The magnetic properties have a close relation to the chiralities of the tubes and the concentration of defects. However, the predicted high mobility of adatoms means that they are likely to recombine with vacancies without some kind of stabilizing agent. This is supported by the irradiation of graphite with inert He, where only a very small magnetic signal was measured.[3]

The role of hydrogen in magnetic carbon systems has attracted recent attention. Density functional theory calculations have shown that hydrogen atoms chemically bonded to carbon atoms in defective Rh-C_{60} do trigger ferromagnetic ordering.[16] Experiments show that irradiation with 2.25 MeV protons on highly oriented pyrolytic graphite triggers ferro- or ferrimagnetism, and that the magnetic ordering is stable at room temperature.[3] This experiment provides a possible effective way for the controllable realization of magnetic carboneous material. By first-principles calculations, previous work has investigated several possible structures that may be responsible for the magnetism[17] in proton-irradiated graphite, including several kinds of H-vacancy and H-adatom complexes.

Although there has been some work on the treatment of carbon nanotubes by proton irradiation[18] and hydrogen plasma,[19] no magnetic measurements have so far been performed. Due to the similarity between carbon nanotubes and graphite, we expect that proton-irradiated carbon nanotubes should also exhibit magnetism. Proton irradiation results in C-H bond formation in a carbon nanotube.[18] Collisions of energetic ions with nanotubes give rise to the formation of large numbers of atomic vacancies and carbon interstitials. The protons are most possibly trapped at carbon vacancies and captured by carbon interstitials. Here we report studies of the magnetic properties of carbon nanotubes when the dangling bonds at vacancies are saturated by hydrogen atoms. Our calculations show that semiconducting tubes are more likely to be spin-polarized by H-vacancy complexes than metallic ones. When a hydrogen atom is pinned by a carbon adatom on the nanotube wall, the C-H group contributes one lone electron localized at the carbon adatom, independent of the type of tube.

II. METHODS

The calculations have been performed using the plane wave basis VASP[20,21] code, implementing the spin-polarized density-functional theory (DFT) and the generalized gradient approximation of Perdew and Wang.[22] We have used projected augmented wave (PAW) potentials[23,24] to describe the core ($1s^2$) electrons. A kinetic energy cutoff of 400 eV was found to converge the total energy of our systems to within meV. We used four Monkhorst-Pack k points[25] (Γ point included) for the Brillouin zone integration along the tube axis. The minima in the total energy are found using a conjugate gradient (CG) algorithm. Supercells are constructed with adequate vacuum space in the radial direction of the tubes to avoid the interaction between adjacent tubes. Periodical boundary conditions are applied in the axial direction to simulate infinite length tubes. We have studied five zigzag SWNTs from (6, 0) to (10, 0) and two armchair SWNTs (4, 4) and (5, 5). The unit cell of the zigzag SWNTs consists of six zigzag carbon atoms rings and the length of the unit cell along the axial direction is set to 12.78 Å. The unit cell of the armchair SWNTs consists of five armchair carbon atom rings and the length of the unit cell along the axial direction is set to 12.3 Å.

Armchair SWNTs are predicted to be metallic, and this has been verified by experiments and first-principles calculations.[26–28] The zone-folding model predicts that the zigzag SWNTs with indices ($3m$, 0) would be metallic, where m is an integer.[29] This is because some allowed wave

vectors of $(3m, 0)$ SWNT pass through the corners ($\mathbf{K}_B$) of the hexagonal first Brillouin zone of a graphene sheet on the basis of this simple model [noting that the graphene is semimetal with valence band and conduction band degenerate at only six corners ($\mathbf{K}_B$) of the hexagonal first Brillouin zone]. However, experiments[26] showed that the (9, 0), (12, 0), and (15, 0) SWNTs have small energy gaps. Ouyang *et al.*[26] generalized that the energy gaps of the $(3m, 0)$ zigzag tubes would scale as R^{-2}, where R is the tube radius. This is due to the finite curvature effect of small-diameter SWNTs that induce shifts of the Fermi points of SWNTs from original $\mathbf{K}_B$. However, the properties of these $(3m, 0)$ zigzag SWNTs should be different from the other semiconducting zigzag SWNTs with indices $(3m-1, 0)$ and $(3m-2, 0)$, the wave vectors of which do not pass through the $\mathbf{K}_B$ of the graphene sheet on the basis of the zone-folding model. Usually, the band gap of the $(3m, 0)$ tube is much lower than those of the $(3m-1, 0)$ and $(3m-2, 0)$ tubes.[30] Calculations based on local density functional theory showed that the (6, 0) SWNT is metallic.[27,31] We have calculated the band structures of these seven SWNTs, and found that the perfect (4, 4), (5, 5), and (6, 0) tubes are metallic, while the (7, 0), (8, 0), (9, 0), and (10, 0) tubes are semiconductors. The energy gap of the (9, 0) tube is calculated to be 0.16 eV, in agreement with the value of 0.17 eV obtained by Blase *et al.*,[31] and compares well with the experimental value of 0.08 eV.[26]

III. RESULTS AND DISCUSSION

A. H-vacancy complex

1. "Parallel" and "perpendicular" configurations

Usually, a new bond is formed between two of the three two-coordinated carbon atoms at a vacancy on the SWNT so that a pentagon is formed on the wall of the tube. There are two kinds of such vacancy configurations. According to the orientation of the new C-C bond in the pentagon relative to the axis of the tube, we denote them as "parallel" and "perpendicular" configurations, respectively.[11] In these two configurations there is a dangling bond. Figure 1 shows the structures formed by saturating the dangling bond at the "parallel" and "perpendicular" vacancies on the zigzag and armchair SWNTs, respectively. We denote the "parallel" vacancy and the "perpendicular" vacancy before hydrogen saturation by V-Par and V-Per, and those after hydrogen saturation by HV-Par and HV-Per, respectively. In Table I, the relative energy and the magnetic moment of each H-vacancy complex configuration on the seven SWNTs are given. The energy of the HV-Par configuration of each tube is set as a reference to zero. For the (6, 0) and (7, 0) tubes, the energy differences between the two configurations are very small, only of tens of meV. The HV-Per configuration is the most preferable structure for all the tubes except the (6, 0) tube. The C-H bond length is 1.08 Å. The C-C bonds related to the two-coordinated carbon atoms are elongated from 1.38–1.39 Å to 1.40–1.41 Å after hydrogen saturation. The adsorption energy of the hydrogen atom is in the range of 5.8–6.4 eV for the HV-Par configuration and 4.9–5.4 eV for the HV-Per configuration, respectively.

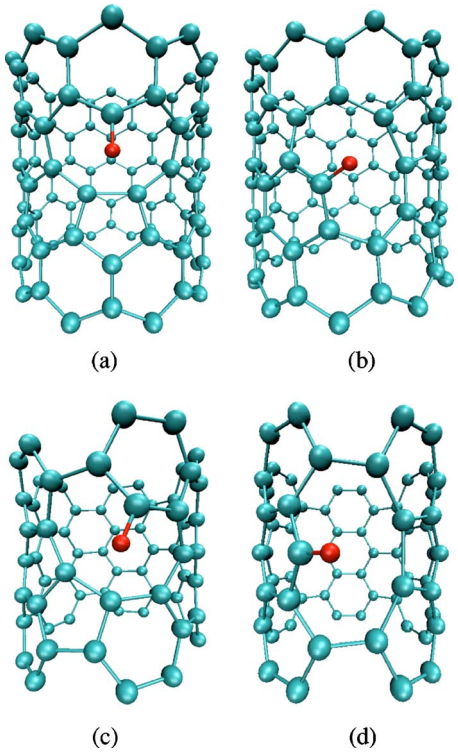

FIG. 1. (Color online) H-vacancy complex structures on the zigzag [(a) and (b)] and armchair [(c) and (d)] SWNTs. (a) and (c) are of the "perpendicular" configuration (HV-Per). (b) and (d) are of the "parallel" configuration (HV-Par). The red spheres represent hydrogen atoms.

The magnetic properties have a close relation to the H-vacancy configuration and the chirality of the SWNT. Only the HV-Per configurations on the (7, 0), (8, 0), and (10, 0) tubes are magnetic, with magnetic moments of 0.9 μ_B, 1.0 μ_B, and 1.0 μ_B, respectively. The magnetic moment originates totally from the delocalized π electrons. Figure 2 gives an example of the distribution of the spin density on the (8, 0) tube. The energies of the paramagnetic ($S=0$) states are 1, 46, and 20 meV higher than those of the ferromagnetic states for the (7, 0), (8, 0), and (10, 0) tubes, respectively.

TABLE I. Relative energies and magnetic moments of the HV-Par and HV-Per configurations on seven SWNTs. The energy of the HV-Par configuration of each tube is set as a reference to zero.

System	HV-Par		HV-Per	
	E (eV)	Mag (μ_B)	E (eV)	Mag (μ_B)
(6, 0)	0.0	0.0	0.06	0.0
(7, 0)	0.0	0.0	−0.08	0.9
(8, 0)	0.0	0.0	−0.20	1.0
(9, 0)	0.0	0.0	−0.29	0.0
(10, 0)	0.0	0.0	−0.29	1.0
(4, 4)	0.0	0.0	−0.22	0.0
(5, 5)	0.0	0.0	−0.48	0.0

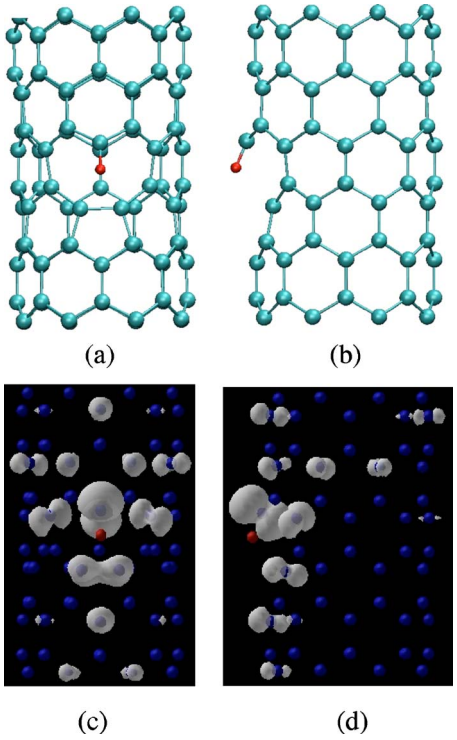

FIG. 2. (Color online) The isosurfaces of the spin density on the (8, 0) SWNT with an HV-Per complex from the front view (c) [structure (a)] and the side view (d) [structure (b)]. The red spheres represent hydrogen atoms.

It seems that only the HV-Per configuration on the semiconducting zigzag SWNTs could exhibit magnetism. At the V-Per vacancy on the zigzag SWNTs, the displacement of the two-coordinated carbon atoms from its original position in the perfect tube is small as is the change of curvature at this atom. The (7, 0), (8, 0), and (10, 0) SWNTs remain semiconducting, while their energy gaps reduce from 0.18, 0.59, and 0.74 eV to 0.14, 0.42, and 0.27 eV, respectively. Figure 3(a) shows the band structure of the (8, 0) SWNT with a V-Per vacancy, for which the gap between the bands $a1$ (HOMO, highest occupied molecular orbital) and $a2$ (LUMO, lowest unoccupied molecular orbital) is 0.42 eV. For these three SWNTs, both the σ electron and π electron of the two-coordinated carbon atom contribute nothing to the HOMO. The HOMO is totally occupied by the π electrons of the other carbon atoms. The electrons of the two-coordinated carbon atom begin to appear in the band just below the HOMO. The saturation of the dangling bond by hydrogen will have little disturbance on the π electron network of the nanotubes. The saturation of the dangling bond produces a new σ bond, leaving an unpaired π electron. This unpaired π electron occupies the LUMO of the (7, 0), (8, 0) and (10, 0) tubes. The LUMOs of these three tubes are flat bands, such as band $a2$ in Fig. 3(a) for the (8, 0) tube. The LUMO splits into two branches, i.e., spin-up and spin-down. The spin-up branch is completely filled, while the spin-down branch is empty for the (8, 0) and (10, 0) SWNTs. The magnetic moments of these two tubes are exactly 1.0 μ_B. The (8, 0) and (10, 0) tubes remain semiconducting. The gaps between the spin-up and the spin-down branches are 0.11 and 0.03 eV for the (8, 0) and (10, 0) tubes, respectively. However, a small quantity of electrons ($\sim$0.05) appear in the spin-down branch of the (7, 0) tube, while the remaining electrons ($\sim$0.95) occupy the spin-up branch. The magnetic moment of this tube is 0.9 μ_B.

Figure 3 shows the evolution of the band structure of the (8, 0) tube from V-Per to HV-Per. For the tube with V-Per, the gap between the bands $a2$ (LUMO) and $a1$ (HOMO) is 0.42 eV. Band $a2$ is a flat band. After the saturation of the dangling bond by a hydrogen atom, the band $a2$ splits into two branches, $b2$-*up* and $b2$-*down*. The band $b2$-*up* is completely occupied while the band $b2$-*down* is empty. As described above, the electrons of the two-coordinated carbon atom at the V-Per on the (8, 0) tube do not contribute to the HOMO, and the saturation of the dangling bond will only influence the valence bands below HOMO. From Figs. 3(a) and 3(b), we can see that the bands $b1$-*up* and $b1$-*down* split from the band $a1$ are nearly of the same shape as band $a1$, while there is large rearrangement among the bands below HOMO. If an extra electron is doped into this system, i.e., the system charged negatively, this electron will occupy band $b2$-*down*. This electron suppresses the spin polarization. The extra electron is distributed around the vacancy and strengthens the bond in the pentagon. The tube becomes nonmagnetic again with a band gap of 0.18 eV [see Fig. 3(c)].

It has been proven that the zigzag tubes and the (4, 4) tube with V-Par vacancy, the (6, 0) tube, and the (5, 5) tube with V-Per vacancy are metallic.[11] The saturation of the dangling bond by hydrogen does not change the metallic character. The (4, 4) SWNT and the (9, 0) SWNT with V-Per vacancy and the (5, 5) SWNT with V-Par vacancy are calculated to be semiconducting.[11] The saturation of the dangling bond by

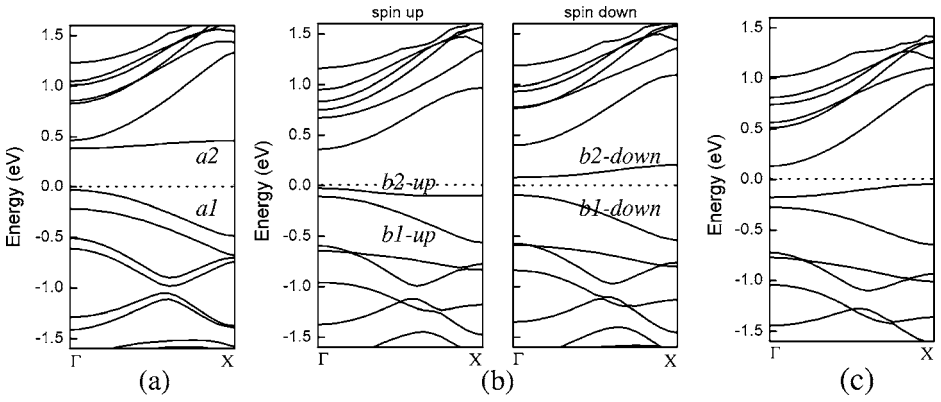

FIG. 3. (a) The band structure of the (8, 0) SWNT with a "perpendicular" vacancy (V-Per). (b) The band structure of the (8, 0) SWNT after the dangling bond at the "perpendicular" vacancy is saturated by a hydrogen atom (HV-Per). (c) The band structure of the (8, 0) SWNT after an extra electron is doped into the HV-Per vacancy.

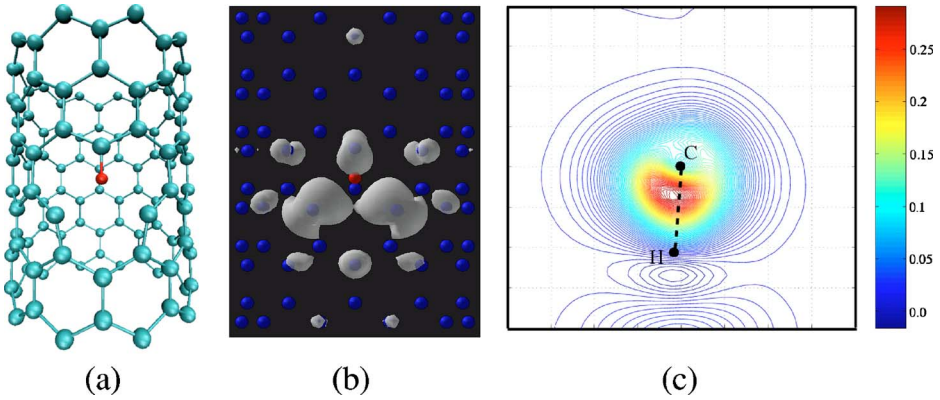

FIG. 4. (Color online) (a) The structure of the 1Ha H-vacancy complex on the (10, 0) SWNT and (b) the isosurface of the spin density. (c) The spin density contour projected on the plane formed by the C-H bond and the axis of the tube. The red spheres represent hydrogen atoms.

hydrogen converts them to metals. In these metallic tubes, the unpaired π electron after the introduction of hydrogen cannot trigger spin polarization.

2. "3db" configuration

Besides the "parallel" and the "perpendicular" configurations, there is another possible configuration for the vacancy on the (10, 0) SWNT. This is denoted "3db," where no new bond is formed at the vacancy and where there are three dangling bonds belonging to the three two-coordinated carbon atoms. This configuration is ferrimagnetic with the net magnetic moment of 1.9 μ_B for the (10, 0) tube.[11] It is a metastable state, with the energy 1.91 eV higher than the ground state (V-Per). This configuration has three dangling bonds, so up to three hydrogen atoms can be adsorbed at this vacancy. We have studied four kinds of H-vacancy structures that may form at the "3db" vacancy, as shown in Figs. 4 and 5. We denote the structures in Fig. 4(a) and Figs. 5(a), 5(c), and 5(d) by 1Ha, 2Ha, 2Hc, and 3Hd, respectively. If the energy of the "3db" vacancy is set as a reference to zero, the energies of the 1Ha, 2Ha, 2Hc, and 3Hd are −4.56, −10.28, −10.73, and −16.03 eV, respectively.

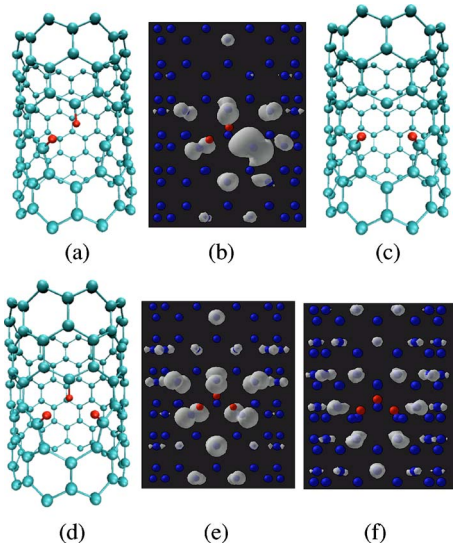

FIG. 5. (Color online) The structures of the 2Ha (a), 2Hc (c), and 3Hd (d) H-vacancy complexes on the (10, 0) SWNT. The isosurfaces of spin density of the 2Ha (b), the positive (e), and negative (f) spin density of the 3Hd. The red spheres represent hydrogen atoms.

The energy of structure 1Ha is 2.32 eV higher than that of the HV-Per. The magnetic moment of this structure is 3.0 μ_B. The 3.0 μ_B comes from the σ electrons of the two dangling bonds, the π electrons, and the $1s$-sp^2 bond between the hydrogen atom and the carbon atom [see Fig. 4(b)]. Each of them contributes 1.8 μ_B, 1.0 μ_B, and 0.2 μ_B, respectively. The spin polarization of the $1s$-sp^2 bond is similar to that for the hydrogen-saturated vacancy in graphite.[17,32] The distance between the hydrogen atom and the two-coordinated carbon atoms is 1.90 Å. At this distance, the electrostatic interaction between the dangling bonds and the hydrogen atom is not negligible. In fact, this interaction has elongated the C-H bond to 1.11 Å, 0.03 Å longer than the typical length mentioned above. Part of the $1s$ electron of the hydrogen atom is attracted toward the side of the dangling bonds. The $1s$ electron participating in the C-H bond is not enough to pair the σ electron of the sp^2 bond of the carbon atom. Part of the σ electron is spin polarized. This can be clearly seen from Fig. 4(c), which shows the spin density contour projected on the plane formed by the C-H bond and the axis of the tube. This kind of H-vacancy complex triggers 3.0 μ_B and 2.3 μ_B magnetic moment in Rh-C_{60} (Ref. 16) and graphite,[17] respectively. In Rh-C_{60}, the π electrons are spin-polarized, but not in graphite.

The configuration 2Hc [Fig. 5(c)] is 0.45 eV more stable than the 2Ha [Fig. 5(a)]. The 2Ha configuration has a magnetic moment of 2.0 μ_B, of which half comes from the dangling bond and half from the π electrons [see Fig. 5(b)]. The energy of the paramagnetic state of the 2Ha is 12 meV higher than that of the ferromagnetic state. The 2Hc configuration is nomagnetic. Both of them are semiconducting, with band gaps of 0.13 and 0.54 eV for 2Ha and 2Hc, respectively. The 2Ha (2Hc) configuration is similar to the V-Par (V-Per): both have the same dangling bonds and the same numbers of π electrons. There is also some similarity in the magnetic properties. Both 2Ha and V-Par have spin-polarized dangling bonds, while the dangling bonds of both 2Hc and V-Per are nonmagnetic.

The ground state of the 3Hd configuration is of ferrimagnetic order. Figures 5(e) and 5(f) show the distribution of the positive and negative spin densities, respectively. The ferrimagnetic state of the 3Hd is 17 meV lower in energy than the paramagnetic state. The magnetic moment of the ferrimag-

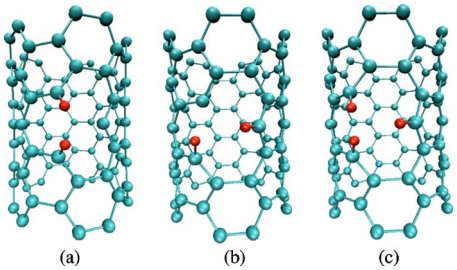

FIG. 6. (Color online) H-vacancy complex structures on the (5, 5) SWNT with two [(a) and (b)] and three (c) hydrogen atoms. The red spheres represent hydrogen atoms.

netic state is 1.0 μ_B. The ratio of the positive magnetic moment to the negative one is about 7:1. The spins at the three carbon atoms bonded with the hydrogen atoms are all positive. The ground state of 3Hd is semiconducting, with a band gap of 0.07 eV.

We have also studied the cases where two or three hydrogen atoms are adsorbed at the vacancy on the (9, 0) and (5, 5) (see Fig. 6) SWNTs. For the (9, 0) tubes, only the structure 2Ha has a magnetic moment of 0.3 μ_B, while the structures 2Hc and 3Hd are nonmagnetic. The magnetic moment of 2Ha comes totally from the dangling bond. There are no spin-polarized π electrons like those of the structure 2Ha on the (10, 0) tube. For the (5, 5) tube, all the structures in Fig. 6 are nonmagnetic.

From the above results, it seems that semiconducting zigzag SWNTs with indices $(3m-1, 0)$ and $(3m-2, 0)$ [(7, 0), (8, 0), and (10,0)] are much more likely to be spin polarized by hydrogen at vacancies than the metallic armchair SWNT [(6, 0), (4, 4), and (5, 5)] and semiconducting SWNTs with indices $(3m, 0)$ [(9, 0)]. The semiconducting property of the former tubes ensures the spin polarization after the dangling bond being saturated by hydrogen.

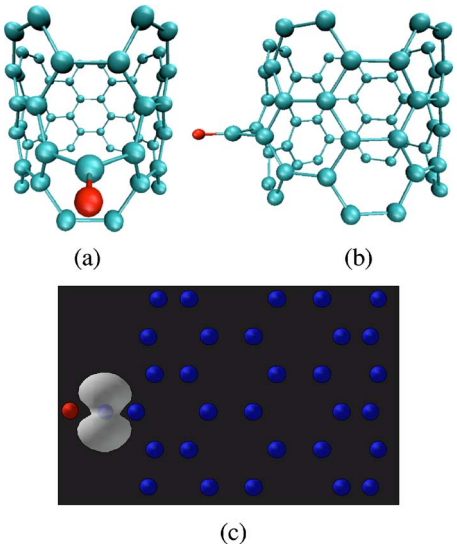

FIG. 7. (Color online) The front view (a) and the side view (b) of the (5, 5) SWNT with a carbon adatom of which one dangling bond is saturated by a hydrogen atom. (c) The side view of the distribution of the spin density that is highly localized at the carbon adatom. The red spheres represent hydrogen atoms.

B. H adatom

The properties of carbon adatoms on the surfaces of graphite and carbon nanotubes have been studied extensively.[6,10] The magnetic moments induced by the adatoms depend strongly on the diameters and chiralities of the tubes and the adsorption sites, and vary from 0.45 μ_B on the graphite surface to 0.0 μ_B on the (7, 0) SWNT surface. If the dangling bond of the adatom is saturated by a hydrogen atom, as shown in Fig. 7 for the (5, 5) tube, we find that the magnetic moment is always 1.0 μ_B, from graphite to small-diameter SWNTs. The spin polarization is highly localized at the carbon adatom, as shown in Fig. 7(c). The ferromagnetic states are 0.25 and 0.35 eV lower in energy than the paramagnetic state for the (5, 5) tube and graphite, respectively.

For the structure in Fig. 7(a), three valence electrons of the carbon adatom participate in the formation of two σ bonds with two carbon atoms of the tube and one σ bond with the hydrogen atom. The remaining electron occupies the p_z orbital perpendicular to the plane formed by these three σ bonds. This p_z orbital is perpendicular to the p_z orbital of the carbon atoms of the substrate. The electron on this p_z orbital is a lone electron, which induces a 1.0 μ_B magnetic moment. This property is independent of the diameter or chirality of the tube.

IV. SUMMARY

First-principles calculations have been used to study the possible structures that may induce spin polarization by hydrogenated carbon nanotubes. Hydrogen trapped at a vacancy can trigger delocalized π electron spin polarization on semiconducting zigzag SWNTs. The semiconducting character of the tubes plays an important role in the spin polarization. Metallic SWNTs are usually not spin polarized by H-vacancy complexes. The H-adatom complex formed by a carbon adatom and a hydrogen atom has a magnetic moment of 1.0 μ_B localized at the carbon adatom on graphite and SWNTs, which is independent of the type of SWNT. Considering both H-vacancy and H-adatom complexes, it seems that semiconducting zigzag SWNTs are superior to metallic SWNTs as candidates for magnetic materials.

The above results are obtained from effectively infinite length nanotubes with defects at a linear density of about 0.08 $Å^{-1}$. If we consider a tube of finite length, such as tens of nanometers or even shorter, the tube will convert from 1D bulk behavior to molecular behavior.[33,34] The original continuous band structure reduces to a discrete set of molecular levels. This finite-size effect has been proved to strongly influence the quantum transport properties[35] and magnetic properties[36,37] of nanotubes. Whether such kind of finite-size effect could influence the magnetic properties of hydrogen-induced defects on nanotubes deserves further investigation.

ACKNOWLEDGMENTS

This research has been supported by the Academy of Finland Centre of Excellence Program (2000–2005) and partially by the ELENA project within the Academy of Finland TULE programme. We are grateful to the Centre of Scientific Computing, Espoo for computational resources.

*Electronic address: yma@fyslab.hut.fi

[1] T. L. Makarova, B. Sundqvist, R. Höhne, P. Esquinazi, Y. Kopelevich, P. Scharff, V. A. Davydov, L. S. Kashevarova, and A. V. Rakhmanina, Nature **413**, 716 (2001).
[2] Y. Shibayama, H. Sato, T. Enoki, and M. Endo, Phys. Rev. Lett. **84**, 1744 (2000).
[3] P. Esquinazi, D. Spemann, R. Höhne, A. Setzer, K.-H. Han, and T. Butz, Phys. Rev. Lett. **91**, 227201 (2003).
[4] A. N. Andriotis, M. Menon, R. M. Sheetz, and L. Chernozatonskii, Phys. Rev. Lett. **90**, 026801 (2003).
[5] Y. H. Kim, J. Choi, K. J. Chang, and D. Tománek, Phys. Rev. B **68**, 125420 (2003).
[6] P. O. Lehtinen, A. S. Foster, A. Ayuela, A. Krasheninnikov, K. Nordlund, and R. M. Nieminen, Phys. Rev. Lett. **91**, 017202 (2003).
[7] K. Kusakabe and M. Maruyama, Phys. Rev. B **67**, 092406 (2003).
[8] M. Fujita, K. Wakabayashi, K. Nakada, and K. Kusakabe, J. Phys. Soc. Jpn. **65**, 1920 (1996).
[9] N. Park, M. Yoon, S. Berber, J. Ihm, E. Osawa, and D. Tománek, Phys. Rev. Lett. **91**, 237204 (2003).
[10] P. O. Lehtinen, A. S. Foster, A. Ayuela, T. T. Vehviläinen, and R. M. Nieminen, Phys. Rev. B **69**, 155422 (2004).
[11] Y. Ma, P. O. Lehtinen, A. S. Foster, and R. M. Nieminen, New J. Phys. **6**, 68 (2004).
[12] S. Okada and A. Oshiyama, J. Phys. Soc. Jpn. **72**, 1510 (2003).
[13] M. S. Ferreira and S. Sanvito, Phys. Rev. B **69**, 035407 (2004).
[14] F. Banhart, Rep. Prog. Phys. **62**, 1181 (1999).
[15] A. V. Krasheninnikov, K. Nordlund, and J. Keinonen, Phys. Rev. B **65**, 165423 (2002).
[16] J. A. Chan, B. Montanari, J. D. Gale, S. M. Bennington, J. W. Taylor, and N. M. Harrison, Phys. Rev. B **70**, 041403(R) (2004).
[17] P. O. Lehtinen, A. S. Foster, Y. Ma, A. V. Krasheninnikov, and R. M. Nieminen, Phys. Rev. Lett. **93**, 187202 (2004).
[18] B. Khare, M. Meyyappan, M. H. Moore, P. Wilhite, H. Imanaka, and B. Chen, Nano Lett. **3**, 643 (2003).
[19] K. Yu, Z. Zhu, Q. Li, and W. Lu, Appl. Phys. A **77**, 811 (2003).
[20] G. Kresse and J. Furthmüller, Comput. Mater. Sci. **6**, 15 (1996).
[21] G. Kresse and J. Furthmüller, Phys. Rev. B **54**, 11169 (1996).
[22] J. P. Perdew, J. A. Chevary, S. H. Vosko, K. A. Jackson, M. R. Pederson, D. J. Singh, and C. Fiolhais, Phys. Rev. B **46**, 6671 (1992).
[23] G. Kresse and D. Joubert, Phys. Rev. B **59**, 1758 (1999).
[24] P. E. Blöchl, Phys. Rev. B **50**, 17953 (1994).
[25] H. J. Monkhorst and J. D. Pack, Phys. Rev. B **13**, 5188 (1976).
[26] M. Ouyang, J. L. Huang, C. L. Cheung, and C. M. Lieber, Science **292**, 702 (2001).
[27] I. Cabria, J. W. Mintmire, and C. T. White, Phys. Rev. B **67**, 121406(R) (2003).
[28] M. Machón, S. Reich, C. Thomsen, D. Sánchez-Portal, and P. Ordejón, Phys. Rev. B **66**, 155410 (2002).
[29] N. Hamada, S. I. Sawada, and A. Oshiyama, Phys. Rev. Lett. **68**, 1579 (1992).
[30] V. Zólyomi and J. Kürti, Phys. Rev. B **70**, 085403 (2004).
[31] X. Blase, L. X. Benedict, E. L. Shirley, and S. G. Louie, Phys. Rev. Lett. **72**, 1878 (1994).
[32] P. Lehtinen, Ph.D. dissertation, Helsinki University of Technology, Laboratory of Physics, 2005.
[33] A. Rubio, D. Sánchez-Portal, E. Artacho, P. Ordejón, and J. M. Soler, Phys. Rev. Lett. **82**, 3520 (1999).
[34] T. W. Odom, J.-L. Huang, P. Kim, and C. M. Lieber, J. Phys. Chem. B **104**, 2794 (2000).
[35] L. C. Venema, J. W. G. Wildöer, H. L. J. T. Tuinstra, C. Dekker, A. G. Rinzler, and R. E. Smalley, Appl. Phys. Lett. **71**, 2629 (1997).
[36] T. W. Odom, J.-L. Huang, C. L. Cheung, and C. M. Lieber, Science **290**, 1549 (2000).
[37] Y. Luo, C. Verdozzi, and N. Kioussis, Phys. Rev. B **71**, 033304 (2005).